Importance of the sub-processes in solid fuel particle gasification: heat conservation and reaction mechanism

Xiyan Li[*],
Department of Energy Technology
Aalborg University, Aalborg, Denmark
e−mail: xli@et.aau.dk

Chungen Yin, Thomas Condra
Department of Energy Technology
Aalborg University, Aalborg, Denmark
e−mail: chy@et.aau.dk, tc@et.aau.dk

ABSTRACT

The aim of this article is to develop a complete and detailed gasification model for a single solid fuel pellet. Three main objectives are achieved: a modified one-dimensional model using C++ code, a reliable results validation using experimental data from literature and an overview of the detailed one-dimensional model results. This model is based upon the partial differential equations (PDEs) describing continuity, species transport, energy and pressure equations. All the equations are highly coupled and are solved using a central-differential scheme (CDS). A time-marching procedure is based on a fully implicit scheme. Both a grid independent validation and a validation against experimental data are given in the paper. The validation results show good agreement with the experimental data. The temperature profile, the definition of the end of each pyrolysis/gasification stages and the effects of sensible enthalpy are presented. Based on this work, an engineering model can be generated in the future, which will be a novelty in biomass (coal) gasification/pyrolysis/combustion, and will do a great use to industry.

KEYWORDS

Single particle, Gasification, Pyrolysis, Computational fluid dynamics (CFD), Finite volume method (FVM)

INTRODUCTION

As the main energy source of the world, fossil fuels are persistently at the focus of controversy. Due to the declining supply of fossil fuels and the issues related to greenhouse gas emissions, there is an urgent need for alternative energy sources. Biomass is in the public focus, not only because it is sustainable but also because of its environmentally friendly characteristics. According to data report from United Nations Environment Programme, the global CO_2 content at the sea level has increased from 315.71 ppm in 1980 to 410.26 ppm in 2018 [1]. Biomass gasification uses gases such as, steam, air, nitrogen, carbon dioxide, methane or a mixture of these gases as gaseous medium to react with biomass. In this way, the greenhouse gases are recycled and syngas is produced.

In order to make full use of the biomass, research has been done on pyrolysis, gasification and combustion, based on both experimental methods and simulation methods. The experimental methods give a way of describing real reaction phenomenon and gaining a set of practical data, for example,
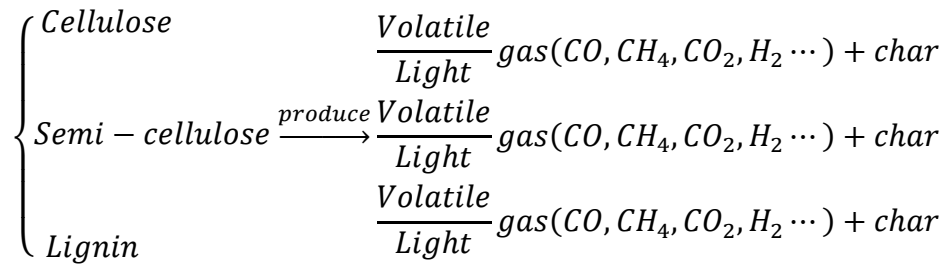
---

[*] Corresponding author

temperature profile, kinetic parameters, reaction order etc., whilst simulation gives a rapid way of looking into the results before experiments or before scale- up is considered. The early research started with crudely measuring the gas components and unreacted carbon and predicting the weight loss value [2]. Laurendeau [3] in 1977 already found out the complete heterogeneous reaction mechanism for coal char and constructed a complete particle reaction model. Limited by the computational capacity at the time, there are not many simulation results, but it still gave a good point for the research that followed. Thurner and Mann [4] put more efforts on the kinetic mechanism of a so-called two-step devolatilization mechanism. Using this mechanism, they compared the composition of gases, tar and residues between experimental data and simulated data. However, no further information about the real gasification results were given. Through the years, the debate about one-step devolatilizaion mechanism and two-step devolatilization mechanism has continued.
One-step global devolatilization mechanism can be described as:

$$Biomass \rightarrow Char + Volatile/Light\ gas(CO, CH_4, CO_2, H_2 \cdots)$$
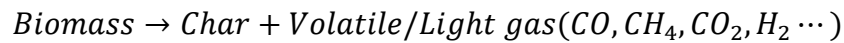
The advantage of one-step global devolatilization mechanism is that the reaction heat is easy to obtain from the measurement of heating value and the composition of the light gas can be easily calculated from the proximate and ultimate analyses. Therefore, the predicted results are reasonably transparent. The difficulty lies in finding a global reaction mechanism data for this reaction. As is known, biomass has complex components and each component has its own reaction mechanism. Perhaps for this reason, some researchers go for the three-parallel devolatilization mechanism or the two-step devolatilization mechanism.
The three parallel devolatilization mechanism is shown simply as:

$$\begin{cases} Cellulose & \dfrac{Volatile}{Light} gas(CO, CH_4, CO_2, H_2 \cdots) + char \\ Semi - cellulose \xrightarrow{produce} \dfrac{Volatile}{Light} gas(CO, CH_4, CO_2, H_2 \cdots) + char \\ Lignin & \dfrac{Volatile}{Light} gas(CO, CH_4, CO_2, H_2 \cdots) + char \end{cases}$$

The three-parallel mechanism can be seen as three one-global devolatilization mechanisms combined together, but with a much simpler composition of reactants. It makes it easier to finding out the mechanism of devolatilization of every single component. The defect is three reactions need to be considered in the model, which may lead to the experimental error accumulating.
A two-step devolatilization mechanism is based on the three parallel devolatilization mechanism. The idea is also to make the reaction mechanism data easier to measure and calculated. The difference is that the classification starts from the products. A medium product, tar is considered. Tar is generated from the primary decomposition, and then further cracking into gas and char. This mechanism describes better the phenomena that occur during pyrolysis, combustion or gasification. However, tar is an unstable matter. The percentage of tar in the products relies on the experimental conditions. Because of that, it is also not easy to find out the reaction heat of producing tar. There are five reactions that need to be considered in the two-step devolatilization model. If the reaction heat is not properly addressed, the simulation error can be much bigger than using the other two devolatilization mechanisms. This will be discussed later in this paper.
The two-step mechanism model is shown as:

$$Biomass \xrightarrow{produces} \begin{cases} Gas \\ \uparrow \\ Tar \\ \downarrow \\ Char \end{cases}$$
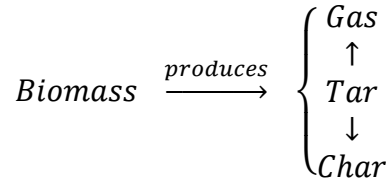
This work is based on a one-dimensional numerical model for the pyrolysis of a single spherical biomass particle. The model is further extended for gasification and combustion. The one-step global devolatilization model is used in this model for its simplicity and accuracy.

METHODOLOGY

The pellet in this model is considered as a one-dimensional spherical fuel pellet, whose properties are isotropic and is under local thermal equilibrium during the heating up process. The CFD model uses central differential scheme with staggered grid for the pressure calculation. The grid number is set to 80. A fully implicit scheme is used a fully implicit scheme for solving the transient term. More details about the partial differential equations are presented below.

The validation experiment is based on data from a sub-bituminous coal (SBC) in a fluidized bed at 850℃ [5][6]. The diameter of the fuel pellet was 10 mm.

Reaction mechanism

Within all the three devolatilization models discussed above, there is one issue has to be considered, and that is to solve the enthalpy of formation of volatile for one-step global devolatilization model and two-step devolatilization model. For the three-parallel devolatilization model, it can be seen as three one-step global devolatilizaiton models combined.

Solid fuel can usually be seen as a combination of moisture, volatile, fixed carbon and ash, as shown in proximate analysis in Table 1. The heating value in the proximate analysis can be treated as the sum of the heating values of the carbon and the volatile. Depending on the form of water when the heating value is measured, the heating value can be classified as lower heating value (LHV) or higher heating value (HHV). In the model that is discussed in this paper, the moisture is treated separately. Therefore, the heating value of volatile is calculated as:

$$HHV_{Volatile} \times \%_{Volatile} + HHV_{Char}\%_{Char} = HHV_{Proximate} \tag{1}$$

$$Volatile \ + \ O_2 \ \rightarrow \ CO_2 \ + \ H_2O + N_2 + SO_2 + \cdots + HHV_{Volatile} \tag{2}$$

$$h^0{}_{Volatile} = h^0{}_{CO_2} + h^0{}_{H_2O} + h^0{}_{N_2} + h^0{}_{SO_2} + \cdots + HHV_{Volatile} - h^0{}_{O_2} \tag{3}$$

$HHV_{Volatile}$ represents the heat that released when the volatile is oxidized completely, and water vapor is still in gaseous state. Equation (3) shows the calculation of enthalpy of formation of the volatile.

Table 1: Proximate analysis, ultimate analysis and heating value [5][6]

Fuel	Moisture[%, a.d]	Volatile[%, a.d]	FC[%, a.d]	Ash[%, a.d]	HHV[kJ/kg, a.d]
Sub-bituminous coal	5.07	21.08	49.93	23.90	31490
	C[%, d.b]	H[%, d.b]	O[%, d.b]	N[%, d.b]	S[%, d.b]
	83.58	4.68	9.2	1.74	0.8

The composition of the volatile can be calculated through the proximate analysis and the ultimate analysis. Table 1 shows an example of these values, including heating values of a sub-bituminous coal particle. Referring to the reference cited in this table [5][6], it is also easy to see that these values can be different depending on the sample even though using the same fuel type.

The calculation of volatile is therefore straightforward, since carbon only exist in the volatile and in the fixed carbon according to the proximate analysis in Table 1. So for a formula of a volatile molecular, $C_xH_yO_zN_wS_v$, the stoichiometry of carbon can be calculated as:

$$x = \frac{C-FC}{Volatile}/M_C \tag{4}$$

H, O, N, S only exist in volatile. Similarly, y, z, w, v can be calculated. Taking the example from Table 1, the volatile can be expressed as: $CH_{4.2197}O_{0.5226}$ after normalization and ignoring N and S. This molecular with a molecular weight of 26.9343 kg/kmol and the enthalpy of formation of -34527 kJ/kg, will be used as input for the validation.

Volatile can be treated as artificial components in the numerical model or can be broken down into real species (such as CO, CO_2, CH_4, C_2H_6, . . .). In the case we study here, it is not easy to break down the volatile into real species, therefore, an artificial component is used to represent volatile in the model, as shown in Table 2.

Table 2: Chemical reactions and reaction rate

index	Chemical reactions	Rate expression	Ref
1	Biomass → Volatile + Char	$r_1 = \partial\rho_{vol}/\partial t = k_1(\rho_{vol,\infty} - \rho_{vol})$	[7]
2	H_2O (free) → H_2O (g)	$r_2 = S_a \frac{h_T(T_j - T_{ini}) + \varepsilon\sigma(T_j{}^4 - T_{ini}^4)}{\Delta h_{evap}}$	
3	H_2O (bound) → H_2O (g)	$r_3 = A_{evp}exp\left(-\frac{E_{evp}}{RT}\right)$	
4	$C + \alpha O_2 \to 2(1-\alpha)CO + (2\alpha - 1)CO_2$	$r_4 = \partial C_{O_2}/\partial t = s_{a,char}[\rho_C/(\rho_C + \rho_B + \rho_A)]k_4 C_{O_2}$	[8]
5	$C + H_2O \to H_2 + CO$	$r_5 = \partial C_{H_2O}/\partial t = s_{a,char}[\rho_C/(\rho_C + \rho_B + \rho_A)]k_5 C_{H_2O}$	[8]
6	$C + 2H_2 \to CH_4$	$r_6 = \partial C_{H_2}/\partial t = s_{a,char}[\rho_C/(\rho_C + \rho_B + \rho_A)]k_6 C_{H_2}$	[8]
7	$H_2 + 1/2O_2 \to H_2O$	$r_7 = \partial H_2/\partial t = k_7 C_{H_2} C_{O_2}^{0.5}$	[9]
8	$CO + 1/2O_2 \to CO_2$	$r_8 = \partial C_{CO}/\partial t = k_8 C_{CO} C_{O_2}^{0.25} C_{H_2O}^{0.5}$	[9]
9	$CO + H_2O \to CO_2 + H_2$	$r_9 = \partial C_{CO}/\partial t = k_9 C_{CO}^1 C_{H_2O}^1$	[9]
10	$CH_{4.2197}O_{0.5226} + 1.29365O_2 \to CO + 2.10985H_2$	$r_{10} = \partial C_{CH_{4.2197}O_{0.5226}}/\partial t = k_{10} C_{CH_{4.2197}O_{0.5226}}^{0.2} C_{O_2}^{1.3}$	[10]

Table 2 shows all the reactions used in this model. The first is the devolatilization mechanism as mentioned previously. The second and the third are the mechanisms for free water and bound water. It should be notice that the free water is only considered when the FSP is over 30% [11]. Reactions 4 to 6, are heterogeneous reactions. It is worth mentioning that the last heterogeneous reaction (reaction 6) does not occur under atmospheric pressure [12] during the gasification temperature. It is presented for reference but not considered in the model because of the relatively low pressure. Reaction 8 to reaction 12 are the homogeneous reactions. The light hydrocarbon here obey the two-step combustion scheme for hydrocarbons proposed by Westbrook and Dryer [13], which are shown as reactions 7, 8,

9, 10 in Table 2. In the two-step mechanism, the main aim is to oxidize volatile and produce CO and H_2, this is the first step. The second step is to gasify CO and H_2, as shown in reactions 7-9.

Table 3 shows the data for the kinetic parameters used in Table 2, calculated from Arrhenius equations with the following expression:

$$k = Ae^{\frac{E_a}{RT}} \tag{5}$$

Table 3: Kinetic data used in this model

Reaction index	Pre-exponential factor (A) [s^{-1}]	Activation energy (E_a) [J/kmol]	Heat of reactions (ΔH) [kJ/kg]
1	3.12×10^5	7.4×10^7	-1376.09
2	-	-	-
3	5.13×10^{10}	8.8×10^7	-2440
4	0.658ᵃ	7.4831×10^7	3950
5	3.42ᵃ	1.297×10^5	-14383.33
6	2083ᵃ	115137	1701.59
7	$10^{12.71}$	1.71×10^5	13435.94
8	2.39×10^{12}	1.702×10^8	10114.28
9	2.75×10^9	8.4×10^7	-12879,38
10	2.119×10^{11}	2.027×10^8	-30420.72

ᵃ Units are m/s⁻¹K⁻¹

Transport equations

For solid species, there is only transient term considered, as show below:

$$\frac{\partial(\rho_i)}{\partial t} = S_i \tag{6}$$

For the gas species, transient term, diffusion term and convective terms are considered, so we have:

$$\frac{\partial(\varepsilon\rho_g Y_{ig})}{\partial t} + \frac{\partial(\varepsilon\rho_g u Y_{ig})}{\partial r} = \frac{\partial}{\partial r}\left(D_{ig}\frac{\partial(\varepsilon\rho_g Y_{ig})}{\partial r}\right) + S_{Y_{ig}} \tag{7}$$

At the inner boundary for solid species, the gradient is set to zero. For the outer boundary, a mass transfer coefficient is used. Therefore a gas film around the pellet is assumed. A reference species and reference temperature are calculated as follows [14].

$$Y_{j,ref} = Y_{j,s} + 1/3\left(Y_{j,\infty} - Y_{j,s}\right) \tag{8}$$

$$T_{ref} = T_s + 1/3\left(T_\infty - T_s\right) \tag{9}$$

$Y_{j,ref}$ and T_{ref} here are used for calculating the gas properties in the gas film. Once the dimensionless parameters, such as, Re, Nu, Sh, Pr are determined, h_M and h_T can be calculated using the following equations.

$$Sh \equiv \frac{h_M L_c}{D_g} = 2.0 + 0.6Re^{\frac{1}{2}}Sc^{\frac{1}{3}} \tag{10}$$

$$Nu \equiv \frac{h_T L_c}{k_g} = 1.05 + 0.6Re^{0.65}Pr^{0.33} \tag{11}$$

The outer boundary for mass transfer can be expressed as:

$$DA \frac{Y_B - Y_P}{\frac{\Delta x}{2}} = A_s h_M (Y_\infty - Y_B) \tag{12}$$

For pressure calculations, considering that the pressure inside the pores of coal/biomass will not change dramatically, the Darcy Law is applied here:

$$\vec{u} = -\frac{\eta}{\mu} \nabla P \tag{13}$$

Continuity equations are combined to solve both velocity and pressure:

$$\frac{\partial (\varepsilon \rho_g)}{\partial t} + \frac{\partial (\varepsilon \rho_g u)}{\partial r} = S_g \tag{14}$$

The most commonly used energy equations are written in terms of temperature, as shown in equation (15). The use of this form of transport equation is advantageous because it not only takes into account the heat of reactions, but also a sum of sensible enthalpy caused by temperature increase within the fuel pellet. By using one-step global devolatilization model, the only uncertainty in equation (15) is the enthalpy of formation of volatile, which can be calculated by knowing the heating value of the solid fuel pellet.

$$\frac{\partial (\varepsilon \rho_g C_{pg} T + \rho_s C_{ps} T)}{\partial t} + \frac{\partial (\varepsilon \rho_g u C_{pg} T_g)}{\partial r} = \frac{\partial}{\partial r} \left(k_{eff} \frac{\partial T}{\partial r} \right) + S_T \tag{15}$$

$$S_T = -\sum_{k=1}^{N} h_{f,k}^0 \dot{w}_k - \sum_{k=1}^{N} h_{f,k} \dot{w}_k = \sum_{k=i}^{N} \Delta H_i \dot{w}_i - \sum_{k=1}^{N} h_{f,k} \dot{w}_k \tag{16}$$

The outer boundary condition for temperature is shown as:

$$k_B A \frac{T_B - T_P}{\Delta r / 2} = A_s h_T (T_\infty - T_B) + A_s \varepsilon \sigma (T_\infty^4 - T_B^4) \tag{17}$$

Besides, for the two-step decomposition model, it was found that the heat of reaction of biomass decomposing into gas, tar and char can be very different, varying from -150kJ/kg [15] to -418kJ/kg [16]. The heat of reaction of intermediate product (tar) cracking and reforming is also not easy to determine, shown in literature from around 42kJ/kg [17] to 50kJ/kg [18] by somehow modified. In the case of three-step parallel model for biomass, the enthalpy of formation of lignin, cellulose, semi-cellulose should be calculated separately, which means the error is accumulated three times by measuring the heating values of these three species separately.

VALIDATION AND RESULTS

Using the model developed above, two validations were made. Both of the experiments are taken from Bu et al [5][6]. The first experiment is based on a 10mm sub-bituminous coal pellet in a fluidized bed with a temperature of 850 ℃. The second experiment uses the same pellet with the same bed temperature, but the atmosphere is changed to 30% oxygen and 70% carbon dioxide. Table 3 shows some properties taken from that experiment.

Table 3: Properties taken from Bu. et al

ρ_{SBC}	$C_{P_{SBC}}$	h_T	T_f
1662	1049	200	1088

K_B	T_{wall}	u_g	D_P
0.6	1123	0.28	10

Figure 1 shows the results of sub-bituminous coal under pyrolysis with nitrogen. The solid line represents the simulated temperature profile at the centre of the SBC pellet. The triangles represent the measured centre temperature results from the experiment. It can be seen that the simulation results follow the experimental investigation. A further determination of pyrolysis stages are shown in Fig. 2.
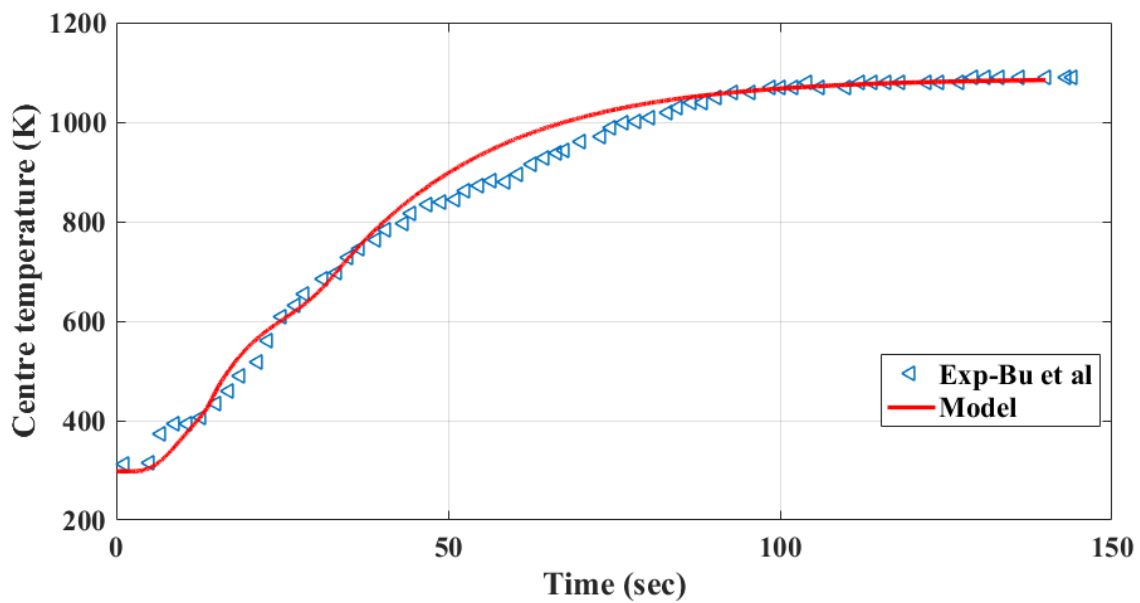

Figure 1 Centre temperature during N_2 pyrolysis calculated by model and measured by Bu et al
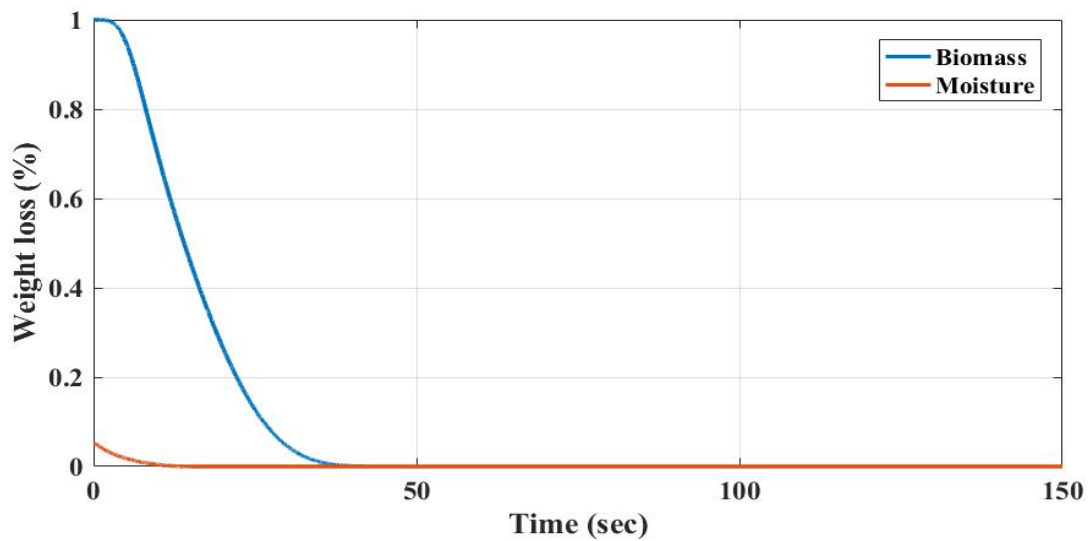

Figure 2 Weight loss profile during pyrolysis

Figure 2 shows the weight loss profile during pyrolysis. Ash is not counted during the calculation, since the mass of ash doesn't change during the pyrolysis process. Water dispears after 14 seconds of reaction. The devolatilization stage is finished after 40 seconds of pyrolysis. In Fig.3, these two stages are shown by arrows.
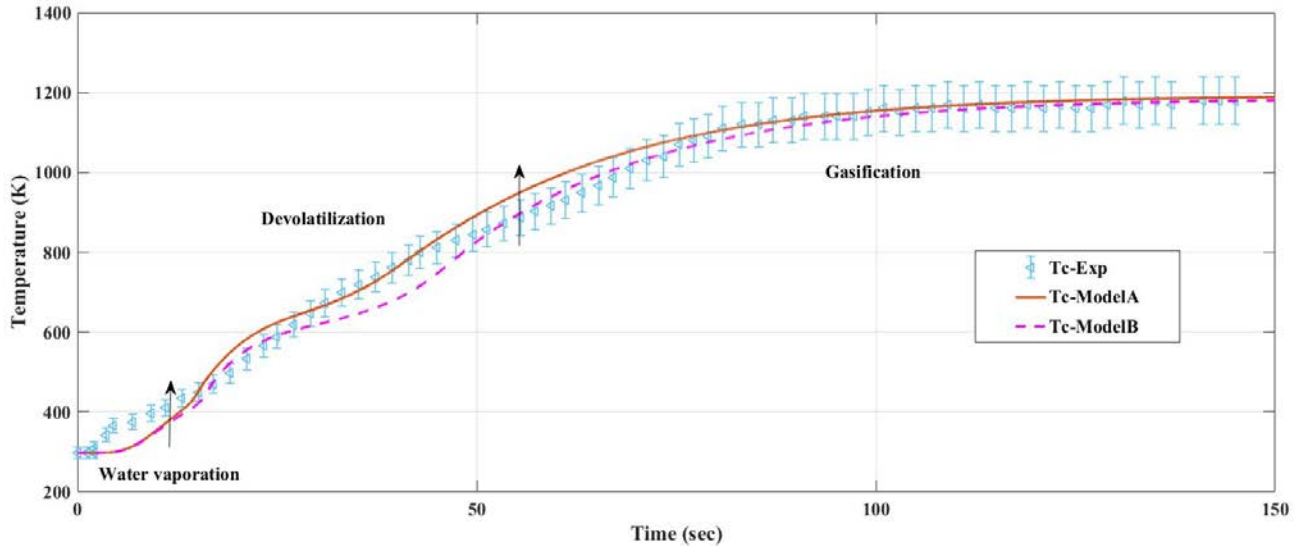

Figure 3 Centre temperature (30% O_2 & 70% CO_2) calculated by model and measured by Bu et al

Figure 3 shows the results of another gasification case, in which the atmosphere of the fluidized bed is changed to 30%$_{vol}$ oxygen and 70%$_{vol}$ carbon dioxide. The solid line shows the simulation result from the model presented in this paper, whereas the dashed line shows the simulation results without considering the sensible enthalpy in the energy equation. The triangles with error bar represents the experimental results from Bu et al [5]. The three stages of the SBC gasification process are marked by arrows. It can be seen that both simulation results agree well with the experimental data. However, considering sensible enthalpy in the energy equation gives a better fit for the temperature at the pellet centre, especially during the devolatilization stage. Sensible enthalpy has negligible effects during the water vaporation stage. In other word, enthalpy of formation is more important than sensible enthalpy during solid fuel pyrolysis, gasification and combustion.

CONCLUSION

This paper describes a detailed gasification model for a sphere solid fuel. Kinetic mechanism, the transport equations, the chemical reactions are considered in the model. A two-step reaction mechanism for volatile gasification is used in this model. A way of calculating the composition of volatile is outlined. Moreover, the mass and heat conservation of a one-step global devolatilization reaction are presented. In the end, two validation results are given. The validation results show the model agrees well with experimental data for both pyrolysis and combustion/gasification processes for a single spherical solid fuel. The gasification validation also shows that energy equation with sensible enthalpy considered agrees better to the experimental results. This work gives a starting point to further investigate a single biomass particle gasification in 2D or 3D, and can serve as a basis for extending the single solid fuel particle to an industrial packed bed gasification/pyrolysis research.

NOMENCLATURE

A_s	The surface area [m^2]
A	Pre-exponential factor [s^{-1}]
E_a	Activation energy of water evaporation, [J/Kmol].
C_P	Specific heat [J/(kg·K)]
$D_{eff,fw}$	Free water effective mass diffusivity [m^2/s]
FSP	Fiber saturation point, %
Δh_{evap}	Latent heat of vaporation [J/kg]
h_f^0	Enthalpy of formation [J/kg]
ΔH	Heat of reactions [J/kg]
h_T	Heat transfer coefficient [W/(m^2·K)]
h_M	Mass transfer coefficient [m/s]
K_B	The thermal conductivity [W/(m·K)]
k_{H_2O}	Reaction rate constant [s^{-1}]
Nu	Nusselt number
Pr	Prandtl number
R_g	Universal gas constant [J/(mol·K)]
r_i	Reaction rate [J/(mol·K)]
r_{H_2O}	The volumetric vaporization rate [kg/(m^3·K)]
SBC	Sub bituminous coal
Sc	Schmidt number
Sh	Sherwood number
S_T	Source term in energy equation [W/m^3]
S_a	The specific area of the wood particle, 2.26×10^4 [m^2/m^3]
T_{ini}	Initial temperature [K]
T_∞	Ambient gas temperature [K]
T_S	Particle surface temperature [K]
$T_{j,S}$	Particle surface temperature for species j [K]
T_C	Particle centre temperature [K]
T_{evap}	Defined as evaporation point of liquid water [K]
u	Velocity [m/s]
Y_{vap}	The percentage of vapor within all the species,
$Y_{j,ref}$	Reference mass fraction of species j in the gas film around the particle
$Y_{j,s}$	Mass fraction of species j at particle surface
$Y_{j,\infty}$	Mass fraction of species j in the ambient gas
ρ_g	Gas density [kg/m^3]
ρ_{vol}	Remaining volatile in solid [kg/m^3]
$\rho_{vol,\infty}$	Ultimate yield of volatile [kg/m^3]
ρ_{fw}	The free water density at the present time [kg/m^3]
$\dot{w}_k$	Reaction rate
λ	The average conductivity of all the gases in the film [W/(m·K)]
ε	Porosity
μ	Dynamic viscosity [kg/(m·s)]
σ	Boltzmann radiation constant, 5.86×10^{-8} (W/m^2K^4)

i	Number of reactions
g	Gas
k	Number of species
l	Liquid
s	Solid

REFERENCES

1. EDE / UNEPlive n.d. http://geodata.grid.unep.ch/extras/graph_co2_concentration.php (accessed May 28, 2018).
2   Arthur JR. Reactions between carbon and oxygen. *Trans Faraday Soc* 1951;47:164.
3   Laurendeac NM. Heterogeneous Kinetics of Coal Char Gasification and Combustion. *Progress in Energy and Combustion Science* 1978;7:2447–50.
4   Thurner F, Mann U. Kinetic investigation of wood pyrolysis. *Ind Eng Chem Process Des Dev* 1981;20:482–8.
5   Bu C, Liu D, Chen X, Pallarès D, Gómez-Barea A. Ignition behavior of single coal particle in a fluidized bed under O2/CO2and O2/N2atmospheres: A combination of visual image and particle temperature. *Appl Energy* 2014;115:301–8.
6   Bu C, Leckner B, Chen X, Pallarès D, Liu D, Gómez-Barea A. Devolatilization of a single fuel particle in a fluidized bed under oxy-combustion conditions. Part B: Modeling and comparison with measurements. *Combust Flame* 2015;162:797–808.
7   Yang YB, Yamauchi H, Nasserzadeh V, Swithenbank J. Effects of fuel devolatilisation on the combustion of wood chips and incineration of simulated municipal solid wastes in a packed bed. *Fuel* 2003;82:2205–21.
8   Lu H, Robert W, Peirce G, Ripa B, Baxter LL. Comprehensive study of biomass particle combustion. *Energy and Fuels* 2008;22:2826–39.
9   Yin C, Kær SK, Rosendahl L, Hvid SL. Co-firing straw with coal in a swirl-stabilized dual-feed burner: Modelling and experimental validation. *Bioresour Technol* 2010;101:4169–78.
10 Jones WP, Lindstedt RP. Global reaction schemes for hydrocarbon combustion. *Combust Flame* 1988;73:233–49.
11 Sharma A, Pareek V, Zhang D. Biomass pyrolysis - A review of modelling, process parameters and catalytic studies. *Renew Sustain Energy Rev* 2015;50.
12 Klose E, Köpsel R. Mathematical model for the gasification of coal under pressure. *Fuel* 1978;72:714.
13 Dryer FL, Westbrook CK. Simplified Reaction Mechanisms for the Oxidation of Hydrocarbon Fuels in Flames. *Combust Sci Technol* 1981;27:31–43.
14 Yin C. Modelling of heating and evaporation of n-Heptane droplets: Towards a generic model for fuel droplet/particle conversion. *Fuel* 2015;141:64–73.
15 Branca C, Albano A, Di Blasi C. Critical evaluation of global mechanisms of wood devolatilization. *Thermochim Acta* 2005;429:133–41.
16 Chan WCR, Kelbon M, Krieger BB. Modelling and experimental verification of physical and chemical processes during pyrolysis of a large biomass particle. *Fuel* 1985;64:1505–13.
17 Haberle I, Haugen NEL, Skreiberg Ø. Drying of thermally thick wood particles: A study of the numerical efficiency, accuracy, and stability of common drying models. *Energy & Fuels* 2017
18 MG Grønli. A theoretical and experimental study of the thermal degradation of biomass.pdf 1996:339.